AGU PUBLICATIONS

Geophysical Research Letters

Temperature Covariance in Tree Ring Reconstructions and Model Simulations Over the Past Millennium

C. T. M. Hartl-Meier[1] (iD), U. Büntgen[2,3,4] (iD), J. E. Smerdon[5] (iD), E. Zorita[6] (iD), P. J. Krusic[2,7,8] (iD), F. C. Ljungqvist[9,10] (iD), L. Schneider[11] (iD), and J. Esper[1]

[1]Department of Geography, Johannes Gutenberg University, Mainz, Germany, [2]Department of Geography, University of Cambridge, Cambridge, UK, [3]Swiss Federal Research Institute WSL, Birmensdorf, Switzerland, [4]CzechGlobe Research Institute CAS and Masaryk University, Brno, Czech Republic, [5]Lamont-Doherty Earth Observatory, Columbia University, Palisades, NY, USA, [6]Institute of Coastal Research, Helmholtz-Zentrum Geesthacht, Geesthacht, Germany, [7]Department of Physical Geography, Stockholm University, Stockholm, Sweden, [8]Navarino Environmental Observatory, Messinia, Greece, [9]Department of History, Stockholm University, Stockholm, Sweden, [10]Bolin Centre for Climate Research, Stockholm University, Stockholm, Sweden, [11]Department of Geography, Justus Liebig University, Gießen, Germany

Abstract Spatial covariance in the simulated temperature evolution over the past millennium has been reported to exceed that of multiproxy-based reconstructions. Here we use tree ring-based temperature reconstructions and state-of-the-art climate model simulations to assess temporal changes in Northern Hemisphere intercontinental temperature covariance during the last 1000 years. Tree ring-only approaches reveal stronger agreement with model simulations compared to multiproxy networks. Although simulated temperatures exhibit a substantial spread among individual models, intercontinental temperature coherency is mainly driven by the cooling of large volcanic eruptions in 1257, 1452, 1600, and 1815 Common Era. The coherence of these synchronizing events appears to be elevated in several climate simulations relative to their own unforced covariance baselines and in comparison to the proxy reconstructions. This suggests that some models likely overestimate the amplitude of abrupt summer cooling in response to volcanic eruptions, particularly at larger spatial scales.

1. Introduction

Knowledge about past climate variability is important for placing recent warming in a historical context (Atwood et al., 2016; Christiansen & Ljungqvist, 2017; Frank et al., 2010; Masson-Delmotte et al., 2013; Smerdon & Pollack, 2016; Snyder, 2010). Proxy-based climate reconstructions and model simulations are sources for quantifying past climate variability, and both provide insights into Earth system responses to external forcing (solar, volcanic, and orbital) and changes in atmospheric composition (Büntgen et al., 2016; Esper, Büntgen, et al., 2013; Hegerl et al., 2006; Ljungqvist et al., 2016; Masson-Delmotte et al., 2013; Schneider et al., 2015; Schurer et al., 2013, 2014). Investigations specifically focused on the past several millennia provide important information because mean climate conditions are close to those of the present day, providing an ideal test bed for assessing the impact of natural and anthropogenic forcings on climate variability and change (Schmidt, 2010).

One important area of investigation is the comparison between proxy evidence and climate model simulations over the last several millennia. These comparisons are important as a means of evaluating the performance of climate models in terms of their simulated internal variability and responses to radiative forcings (e.g., Braconnot et al., 2012; Harrison et al., 2016; PAGES 2k-PMIP3 group, 2015; Schmidt, 2010; Schmidt et al., 2014; Smerdon et al., 2017). Importantly, paleoclimate evaluations of models that are also used to make projections based on possible future emission pathways, and proxy-model comparisons have direct quantitative relevance for risk assessments. Previous paleoclimate proxy-model comparisons have demonstrated, inter alia, that models can underestimate internal climate variability (e.g., Valdes, 2011), may incorrectly represent external radiative perturbations (e.g., Anchukaitis et al., 2010; Braconnot et al., 2012; Esper, Schneider, et al., 2013; Stoffel et al., 2015), and may represent the dynamics and character of hydroclimate variability with varying degrees of success (e.g., Ault et al., 2014; Coats, Cook, et al., 2015; Coats, Smerdon, Cook, et al., 2015; Coats, Smerdon, Seager, et al., 2015; Landrum et al., 2013 ; Ljungqvist et al., 2016).

Recent work on the consistency between model simulations and proxy-based reconstructions revealed substantially higher temperature covariance across continents in the simulations, compared to the

reconstructions (PAGES 2k-PMIP3 group, 2015). This finding calls into question estimates of spatial covariance in surface temperature fields estimated from either of these approaches: temperature covariance is either too high in the simulations or it is too low in proxy-based reconstructions. The PAGES 2k-PMIP3 group (2015) used continental scale temperature reconstructions derived from multiproxy compilations produced by the PAGES 2k Consortium (2013) (hereafter termed PAGES2k reconstructions). These proxy records include historical documentary data, ice cores, corals, marine and lake sediments, pollen, tree rings, and speleothems. Lower covariance of reconstructed temperatures might be due to different proxy-specific uncertainties inherent in the data, while model simulations contain no such noise and therefore likely higher spatial covariance. Some models, on the other hand, may overestimate forcing responses that could in principal inflate the degree of spatial covariance in model simulations (Schurer et al., 2013; Stoffel et al., 2015). Currently, the level of spatial covariance in surface temperatures and its representation in model simulations and proxy-based reconstructions is uncertain, particularly as assessed over multiple decades or centuries. Assessing this discrepancy using reconstructions derived from only one proxy (tree rings) is one means of helping to understand the mismatch. Furthermore, we assume that periods of high temperature covariance are associated with distinct radiative forcings (Anchukaitis et al., 2017) in modeled as well as reconstructed temperature estimates, and therefore, temporally resolved assessments of spatial covariance can contribute to physically relevant assessments of models and proxy-based reconstructions.

Large volcanic eruptions are the strongest natural forcing of temperature variability over the past millennium at multiyear timescales (Colose et al., 2016; Esper, Büntgen, et al., 2013; Robock, 2000; Sigl et al., 2015). The representation of volcanic-induced cooling in proxy-based reconstructions and model simulations is therefore critical, and the magnitude of the response as represented in proxies and models has been debated (Anchukaitis et al., 2012; Esper, Schneider, et al., 2013; Mann et al., 2012, 2013; Stoffel et al., 2015; Wilson et al., 2016). It has also been demonstrated that models overestimate postvolcanic cooling during the instrumental period (Brohan et al., 2012), but these estimates are based on the limited number of eruptions occurring after the establishment of large-scale instrumental networks. With respect to the very large eruptions (e.g., 1257, 1452, 1600, and 1815) there are still substantial uncertainties about the subsequent temporal and spatial response of the climate system as represented in model simulations and proxy-based reconstructions (Atwood et al., 2016; Fernández-Donado et al., 2013; Ljungqvist et al., 2016; Marotzke & Forster, 2015; Stoffel et al., 2015; Wilson et al., 2016).

In this study, we assess the covariance of reconstructed and modeled summer temperature variability over Northern Hemisphere continents by comparing tree ring-based temperature reconstructions with state-of-the-art model simulations over the past millennium. We evaluate the significance of climatic forcings on the intercontinental summer temperature covariance by matching proxy and model data over the past millennium. We hypothesize that volcanic forcing imposes higher spatial covariance on both the proxy reconstructions and model simulations while more typical internal variability reduces covariance below a detectable threshold.

2. Data and Methods

2.1. Temperature Reconstructions

We use all 36 tree ring-based Northern Hemisphere temperature reconstructions from Esper et al. (2016) that extend back to at least A.D. 1000 (Figure 1a). Regional subdivision of the reconstructions were performed according to the PAGES2k domains (PAGES 2k Consortium, 2013) assigning 9 records to Europe, 11 to Asia, 7 to North America, and 9 to the Arctic (Table S1). Esper et al. (2016) provides a comprehensive description of the underlying tree ring data (updates at www.blogs.uni-mainz.de/fb09climatology/reconranking). In this study, we use only the published temperature reconstructions from the original articles accepting the fact that the methods used by the original authors for transferring tree ring chronologies into temperature units vary substantially, resulting in reconstructions with different amplitudes of variability (Figure S1) (see, e.g., Christiansen & Ljungqvist, 2017; Esper et al., 2005; Tingley et al., 2012; von Storch et al., 2004). Despite these differences, and despite the temperature targets (e.g., maximum or mean temperatures, and seasonality of the proxy signal) the simple arithmetic continental means correlate quite well over the past millennium (see below for details, Figure 1b). Consequently, we refrain from any filtering, smoothing, or
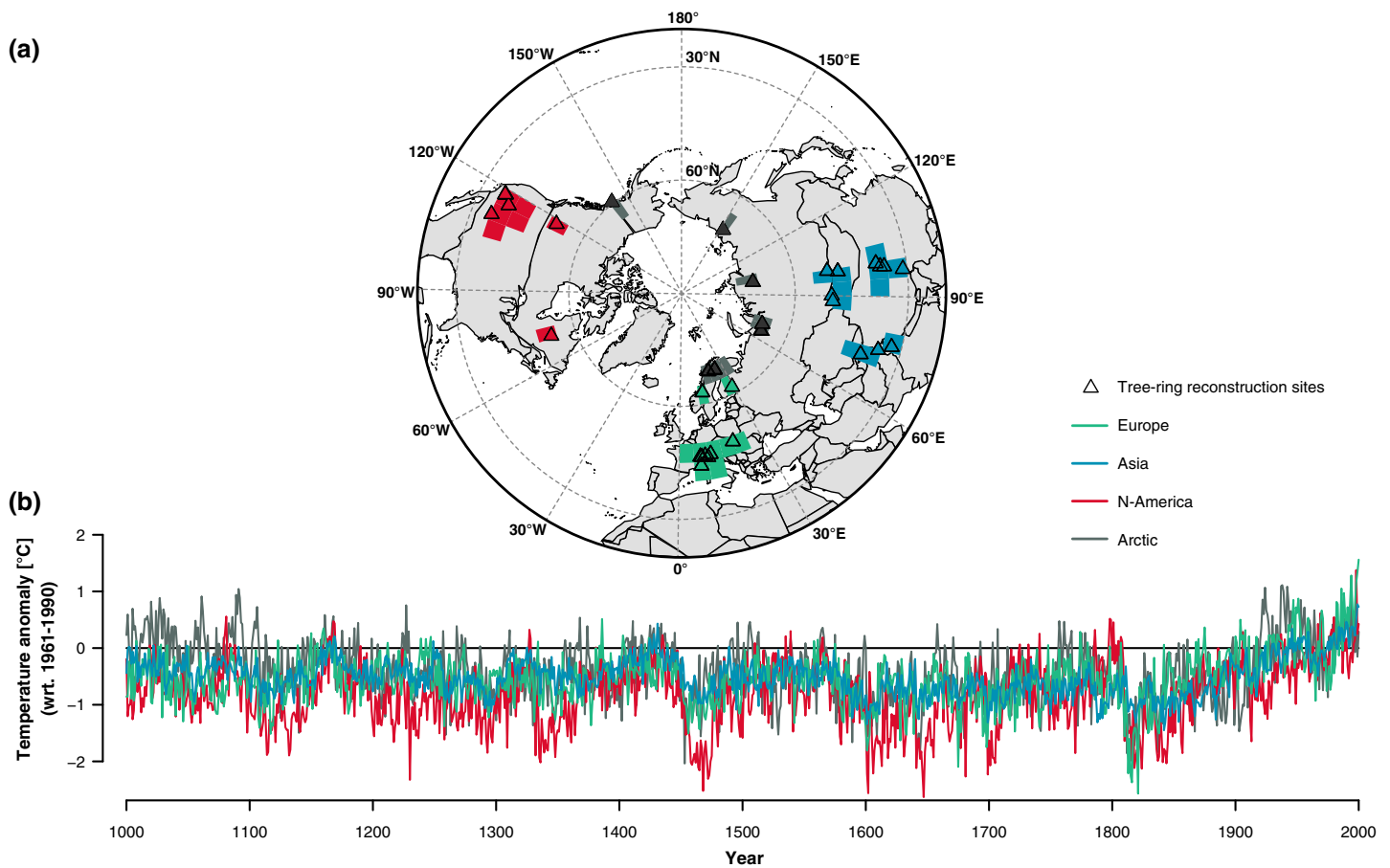
Figure 1. Continental scale tree ring-based temperature reconstructions. (a) Location of the 36 millennium length tree ring reconstructions used in this study (triangles) including 9 records in Europe (green), 11 in Asia (blue), 7 in North America (red), and 9 in the Arctic region (dark grey). The corresponding simulation grid cells are filled with matching colors. (b) The arithmetic mean curves computed for each continent from the subset reconstructions, expressed as temperature anomalies with respect to 1961–1990 for Europe (green), Asia (blue), North America (red), and the Arctic (dark grey).

standardization of the data and instead center all reconstructions such that they represent temperature anomalies relative to the 1961–1990 reference period.

We are aware that the "Arctic," as used here, does not represent a continent but use "continental scale" according to the PAGES2k terminology (PAGES 2k Consortium, 2013). We also concede that the simple arithmetic mean time series are not truly "continental scale temperature reconstructions." Nevertheless, we apply a parsimonious data treatment and herein use the terminology "continental (scale) reconstructions" despite the fact that the records are not fully integrating temperature patterns at continental scales but have particular clustered geographic distributions within a continent (Figure 1).

We also use the PAGES 2k Consortium (2013) multiproxy temperature reconstructions for Northern Hemisphere continents for comparison, although we exclude the North American reconstructions due to their low temporal resolution (30 years). It is also noted that the PAGES2k Europe and Arctic records share reconstructions from central and northern Scandinavia (PAGES 2k Consortium, 2013) and that we used the updated Arctic reconstruction (McKay & Kaufman, 2014).

2.2. Model Simulations and Instrumental Data

We use five last-millennium (850–1849 Common Era (C.E.)) simulations from phase 3 of the Paleoclimate Modeling Intercomparison Project (PMIP3) (Schmidt et al., 2011) appended to the first ensemble member of the historical simulations (1850–2005 C.E.) from phase 5 of the Coupled Model Intercomparison Project (CMIP5) (Taylor et al., 2012) (see Table S2 for details). All model output is interpolated to a common 5° × 5° latitude-longitude grid, allowing a straightforward comparison between the different model fields. For

instrumental data, we use HadCRUT4 (Morice et al., 2012) infilled by kriging (Cowtan & Way, 2014) to avoid data gaps.

Because the tree ring temperature reconstructions are unevenly distributed over the continents, we used the 36 grids containing the proxy locations to calculate means from the simulations and instrumental data (Figure 1a and Table S1). This procedure ensures consistent replication and spatial representation of the continental means from the reconstructed, simulated, and instrumental temperature data sets. To evaluate potential sampling biases, however, additional calculations were performed with representative continental means, i.e., including all grid points on the continents for instrumental and simulated data (see Table S3). Because 28 out of 36 tree ring reconstructions represent summer temperatures (Esper et al., 2016), we derive June–August (JJA) mean temperatures for the modeled and instrumental data, all of which are represented as anomalies relative to the 1961–1990 reference period.

2.3. Covariance Analysis

Intercontinental covariance of the observed, reconstructed, and simulated temperatures was quantified using Pearson's correlation coefficients calculated over the A.D. 1000–2000 and 1850–2000 intervals. Intracontinental covariance was computed as the average correlation of point-to-point time series within a continent. The association among continental means was additionally assessed by calculating the between-series correlations over 31 year moving windows. For comparison, the same calculations were performed over the last 500 years of preindustrial control simulations for each of the employed PMIP3/CMIP5 models, with the understanding that the upper 95% confidence limit of the overall control simulation covariances is considered the baseline for distinguishing unforced background covariance of the multimodel mean. Setting a baseline for the expected covariance based on model control runs, i.e., constant forcing conditions, helps to detect extraordinary or large-scale radiative forcing-induced covariance shifts. Temporal changes in variances of simulated and reconstructed temperature records were calculated using 31 year running standard deviations. All calculations were performed using unfiltered temperature anomalies, i.e., including the full spectrum of interannual variability.

3. Results and Discussion

3.1. Spatial Covariance

In the reconstructions and in some simulations, summer temperatures are more heterogeneous at regional scales relative to hemispheric scales (Figure 2). This is evident in the smaller intracontinental correlations between temperature estimates, i.e., the average correlation of temperature variability within a continent, relative to the correlation among continental means. The intracontinental correlations are lowest among the tree ring reconstructions; from 0.17 within Europe and Asia to 0.27 within North America. Within the simulations, the intracontinental correlations are substantially higher, reaching 0.53 in CCSM (Europe) and 0.48 in IPSL (Europe). In both the tree-ring and simulation data, the intracontinental correlations are generally consistently lower in the Arctic and Asian continents relative to Europe and North America. This is likely due to the more widely distributed locations of Arctic and Asian tree ring sites (Figure 1a).

As noted above, the correlations between the continental means are higher than the intracontinental correlations (Figure 2 and Table S4). This is true for both proxy and simulation time series, although differences are less pronounced in the models, which is likely the result of the additional site-specific noise in the proxy estimates; i.e., regional averaging is more relevant for filtering out random noise in the proxy series. The highest intercontinental covariance is found in the CCSM simulation, followed by IPSL, reaching $r \geq 0.41$. The MPI model also shows high intercontinental correlations ($r \geq 0.36$), except in the Arctic. The BCC and GISS simulations display much reduced, and in some cases insignificant, correlations particularly between North America, Asia, and the Arctic (-0.03 to 0.28). In comparison, the PAGES 2k-PMIP3 group (2015) report correlations of modeled temperatures between Europe, Asia, and the Arctic all at >0.7, but that study used 23 year low-pass filtered data that substantially impacts these calculations. The filtering may also explain the much lower covariance of the PAGES2k reconstructions compared to the simulations identified in the earlier study.

The intercontinental covariance between tree ring reconstructions is in the center of the spread of the model simulations. Without smoothing, however, the PAGES2k temperature reconstructions also display lower correlations than the tree ring reconstructions (note the asterisks in Figure 2) indicating that the single-
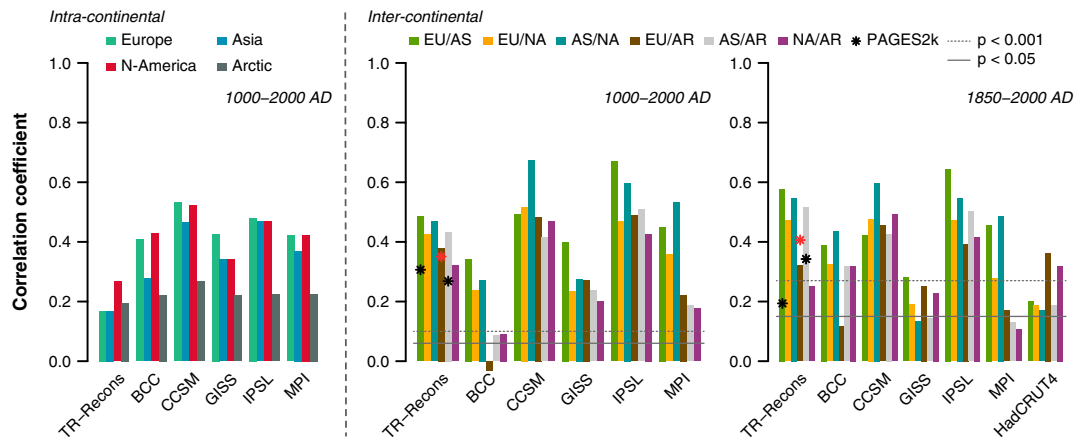
Figure 2. Intracontinental and intercontinental correlations of summer temperatures from tree ring reconstructions and different model simulations from 1000–2000 and 1850–2000. The asterisks represent the corresponding values of the PAGES2k multiproxy reconstructions, and the red asterisks indicate data overlap between continental PAGES2k reconstructions. HadCRUT4 data are available back to 1850.

proxy records from tree rings contain more common variance among the continents than the multiproxy reconstructions. Differences in reconstruction methods and proxy characteristics also likely contribute to lower correlation coefficients (PAGES 2k-PMIP3 group, 2015). The multiproxy approach thus has advantages described elsewhere (e.g., Mann, 2002), but it also seems to include biases from the different proxies in ways that are difficult to assess. For instance, proxy-specific biases and uncertainties are combined in a multiproxy reconstruction by mixing varying seasonal signals and different spatiotemporal resolutions, all of which are regressed onto the same target data using an array of reconstruction methods (Christiansen, 2011; Smerdon et al., 2016, 2011; Tingley et al., 2012; Wilson et al., 2016).

Over the 1850–2000 period (Figure 2, right), the intercontinental correlations are still significant and higher than those calculated over the millennium, even though the degrees of freedom are significantly reduced over the much shorter instrumental period. The correlations are nevertheless expected to be enhanced by the centennial scale warming trend in both the tree ring reconstructions and model simulations (Figures 1b and S1). In contrast, the covariance of the PAGES2k temperature reconstructions between Europe and Asia decrease remarkably (note the asterisks in Figure 2), but the overlap of the time series is also shorter, ending in 1989. The PAGES2k data also yield higher correlations between the Europe and Arctic records over the 1850–2000 period, which is likely due to the data overlap in the reconstructions from northern Scandinavia. The GISS model and HadCRUT4 instrumental data display the lowest covariance, with the instrumental data returning the lowest correlations when including time series from Asia. The latter might be due to data gaps in late nineteenth and early twentieth century data as well as the methods used to infill data. Sparse early instrumental coverage is typical for vast areas in Asia (Morice et al., 2012), and the infilling procedure using kriging techniques (Cowtan & Way, 2014) reduces year-to-year variability and low-frequency trends, particularly before 1880 (Figure S2). The mismatch between observations and simulations, as well as reconstructions, points to a basic challenge in representing large-scale spatial temperature patterns.

3.2. Spatiotemporal Covariance

Running correlations reveal sharp deviations particularly in the model simulations and demonstrate that the above discussed correlations, which are for the most part highly significant, are not stable over time (Figure 3a). There is no clear pattern indicating that a particular pair of continents shows systematically stronger or weaker correlations (Figure S3). The detected temporal covariance patterns do not change (Figure S4a) using full continental means (as specified in Table S3); therefore, they appear to be unaffected by the subsampling of the continental fields.

The temporal agreement of the spatial covariance between modeled and reconstructed temperatures is fairly uniform, particularly since the midfifteenth century (Figure 3a). Prior to the fifteenth century, however, the running correlations of the reconstructions and models diverge substantially, indicating that in some periods the proxy reconstructions yield high temperature covariance among the continents while correlations
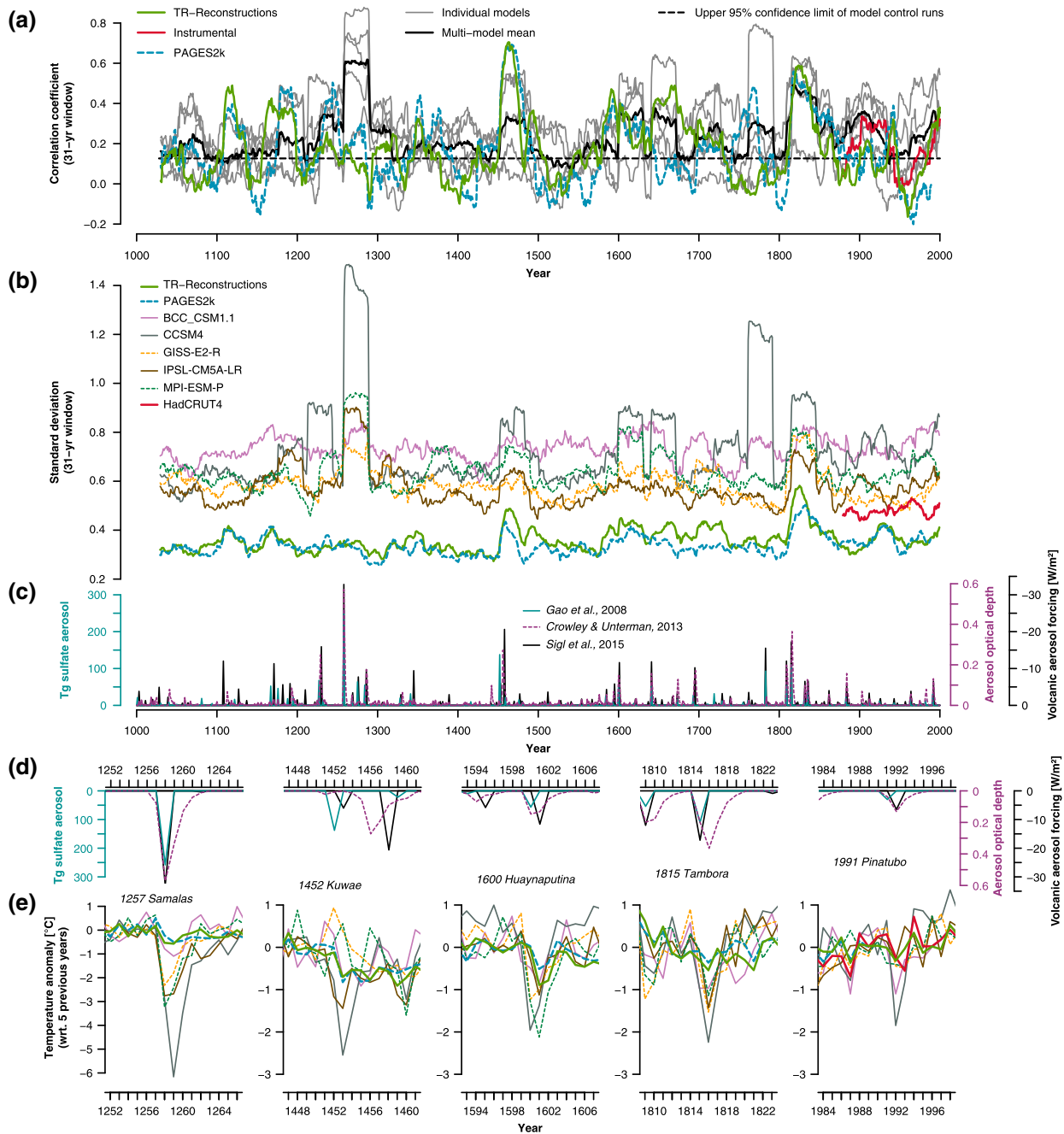
Figure 3. Effects of volcanic forcing on near-surface temperature averaged over Europe, Asia, North America, and the Arctic. (a) Mean intercontinental running correlations (31 year window, left aligned) for tree ring reconstructions (green), PAGES2k reconstructions (blue; note that this includes Europe, Asia, and Arctic only), instrumental data (red), and five model simulations (grey; multimodel mean in black; dashed black line represents upper 95% confidence limit of model control runs as baseline for unforced background covariance). (b) Mean running standard deviation (31 year window, left aligned) of reconstructed, modeled, and instrumental temperature data. Standard deviations were calculated for each continent and then averaged. (c) Volcanic forcing from Crowley and Unterman (2013), Gao et al. (2008), and Sigl et al. (2015). (d) Volcanic forcing and (e) reconstructed and modeled temperature anomalies with respect to the five years prior to assumed dates of the Samalas, putative Kuwae, Huaynaputina, Tambora, and Pinatubo eruptions.

between simulated temperatures drop substantially and vice versa. Interestingly, periods of high and low covariance are also unequal among the models, with only the MPI and GISS simulations showing similar relationships (Figure S3 and Table S5). The agreement in covariance of tree ring and PAGES2k reconstructions is generally higher compared to the models (Table S5), except for the seventeenth century where the tree ring and model patterns cohere well. In this period, both show a simultaneous increase of

correlation coefficients and the values are at a similar magnitude (Figure 3a). While PAGES 2k-PMIP3 group (2015) produced constantly higher correlations with model simulations, compared to the PAGES2k reconstructions, we cannot ascertain a consistent pattern. The higher model values reported in the literature are likely affected by the additional detrending (23 year Hamming filter) of the reconstructed and simulated data (PAGES 2k-PMIP3 group, 2015).

The high coherence periods evident in Figure 3a exceed the background covariance estimated from control simulations (dashed line in Figure 3a) and coincide with major volcanic eruptions affecting both the reconstructions and model simulations, as discussed in more detail below. In the midfifteenth century the reconstructions show the highest correlations, exceeding those derived from the simulations. In subsequent periods, correlations between the reconstructions increase earlier, already in the late sixteenth century, compared to the model simulations in which increases start ∼1600. The curves then cohere well until the present, except for the late eighteenth century when the models indicate much larger spatial covariance. The twentieth century positive trend is mainly caused by the greenhouse gas forcing and associated warming trend. This fact supports our assumption that large-scale radiative forcings increase temperature covariance between continents. The intercontinental correlation among the instrumental data matches the reconstructions more closely than the model simulations, a fact that might be connected to the calibration of the proxies on the instrumental data. Considering the full continental means, however, the covariance of instrumental and modeled data is almost identical (Figure S4a).

3.3. Role of Forcing

Our findings suggest that large-scale radiative forcing imposes higher spatial covariance on continental scale temperature records, while more typical internal variability reduces covariance. As mentioned above, the high covariance periods are induced by volcanic forcing, in both the reconstructed and simulated time series. Anchukaitis et al. (2017) also connected strong radiative forcing due to volcanism to a common spatial forcing of tree ring temperature reconstructions. Interpreting the model control run as background variance (Figures 3a and S5) implies that volcanic eruptions are the dominant radiative forcing over the past millennium, causing spatial covariance shifts in reconstructed and simulated continental temperature records. The models, however, show on average much more abrupt increases of covariance in response to large volcanic eruptions, compared to the more smoothed behavior of the tree ring and multiproxy curves (Figure 3a). These sharp correlation shifts are also missing in the PAGES 2k-PMIP3 group (2015) analysis because the data were smoothed to emphasize decadal or multidecadal patterns prior to covariance assessments.

The spikes in the running correlations are caused by abrupt (single-year) and widespread cooling in simulated temperatures that are forced by large volcanic events (Figure 3). In general, the model simulations display consistently stronger cooling responses compared to the more muted proxy-based reconstructions. These differences might partly be related to the calibration methods used for reconstruction (Esper et al., 2016), as well as the subsampling of continental fields, as the standard deviation decreases when considering full continental mean temperatures. However, the abrupt correlation shift remains in the fully sampled continental means (Figure S4b).

The CCSM model shows the most pronounced response to volcanic forcing including exceptional deviations in 1214, 1258, 1453, 1600, 1641, 1762, and 1815 (Figure 3b). The MPI and IPSL also respond quite strongly to volcanic forcing (particularly in 1258 and 1809/1815), while the BCC and GISS models appear to be less sensitive. Regarding the general pattern of variance changes as well as the level of variance, the IPSL and GISS simulations seem to be closest to "reality" as reflected by the reconstructions and observations. It must be noted, however, that a direct comparison of the level of variance is generally limited as simulated data are free of measurement noise, while proxy data do contain nonclimatic noise that can reduce temperature covariability.

The most severe deviations in the model simulations are driven by volcanic events, though both the magnitude and timing of postvolcanic cooling differ substantially among the models. Part of this difference is related to the forcing time series used in the models (Figures 3d and 3e). The BCC and CCSM models are driven with forcing data from Gao et al. (2008), while the GISS and MPI models used the data from Crowley and Unterman (2013) (Table S2). We here included these two forcing time series (Figures 3d and

3e) together with the recently developed reconstruction by Sigl et al. (2015). The 1257 Samalas eruption was detected in all forcing time series (Crowley & Unterman, 2013; Gao et al., 2008; Sigl et al., 2015) as the largest volcanic event of the past millennium. Consequently, this event produces the strongest cooling in all model simulations, but the cooling magnitude differs substantially among the models. The CCSM simulation produces a maximum cooling of −6.5°C 2 years after the eruption (note the differing scales in Figure 3e). Single grid cells in the CCSM simulation reach −13.5°C post-Samalas cooling exceeding the temperature range of all the other models by far (Figure S1) and lacking any empirical support (e.g., Guillet et al., 2017). BCC shows the least cooling among the models and is closest to the temperature response indicated by the proxy reconstructions.

In other periods, cooling is stronger in the reconstructions, or the annual timing differs among the models. For the yet unknown and thus still intensively researched putative 1452 Kuwae event (Esper et al., 2017), the reconstructions, as well as the Gao et al. (2008) and Ammann et al. (2007) forced models, show cooling in 1453, while the Crowley and Unterman (2013) forced models indicate warming with no sign of cooling until 1456. The 1600 eruption caused simultaneous cooling in all data sets, even though the models again show stronger cooling. In the reconstructions, the cooling following the 1815 Tambora eruption was already started in 1809, following a so far unidentified volcanic event (Cole-Dai et al., 2009; Sigl et al., 2015). The simulated cooling again exceeds the reconstructed postvolcanic cooling. Regarding the 1991 Pinatubo event, some simulations again overestimate the cooling amplitude, and the tree ring reconstructions are actually closer to the instrumental data.

Mann et al. (2012) argued that tree rings underestimate volcanic cooling compared to model simulations and introduced a "missing ring" hypothesis to explain the absence of strong cooling in dendrochronological reconstructions, particularly following the 1257 eruption. This hypothesis has been repeatedly contradicted (see Anchukaitis et al., 2012; D'Arrigo et al., 2013; Esper et al., 2015; St. George et al., 2013; Stoffel et al., 2015; Wilson et al., 2016). Our results indicate the CCSM model, a previous version of which was used in Mann et al. (2012), overestimates volcanic impact. Atwood et al. (2016) also suggests that the relative contribution of volcanic forcing is not adequately represented in past millennium simulations. Because the dating of many eruptions also differs among the forcing time series, these discrepancies add to large uncertainties in evaluating the preinstrumental climate and underlying forcing (Atwood et al., 2016; Esper et al., 2017; Luterbacher et al., 2016). A common forcing for model simulations will thus help comparisons between reconstructed and modeled temperatures (Jungclaus et al., 2016), as will changes in the sensitivity of models to various radiative forcings, including volcanic forcings (e.g., Otto-Bliesner et al., 2016). These continued improvements in model representations of climatic change and variability may eventually reconcile the differences that we note.

Our results also indicate that the temporal and spatial responses of the climate system, as well as the response of proxies to single volcanic events, are still not fully understood (Wilson et al., 2016). We here used 36 tree ring-based temperature reconstructions including 7 records derived from maximum latewood density (Esper et al., 2016), which is known to contain substantially less biological memory compared to tree ring width (Büntgen et al., 2015; Esper et al., 2015, 2017; Schneider et al., 2015, 2017). Maximum latewood density-based temperature reconstructions therefore enable a more accurate estimate of postvolcanic cooling (Schneider et al., 2015, 2017), and the development of such records at large spatial scales is needed to improve our understanding of proper estimates of postvolcanic cooling. This will finally help to enhance our knowledge about the temporal and spatial effects of external radiative forcing and the respective temperature covariance at larger spatial scales.

4. Conclusions

Large-scale radiative forcing increases spatial covariance of continental scale temperatures. This is an important fact to be considered in the combined evaluation of model simulations and proxy-based climate reconstructions and can help to improve our knowledge of natural forcing factors and climate responses. The PAGES 2k-PMIP3 group (2015) showed that model simulations contain a higher degree of spatial temperature covariance at continental scales, compared to the PAGES2k multiproxy reconstructions. Here we show that this intercontinental temperature covariance is higher in tree ring-only reconstructions compared to the multiproxy reconstructions, a finding that narrows the gap between proxy- and model-based spatial

representations. The assessment of temporal covariance changes revealed that periods of high intercontinental coherence are mainly driven by large volcanic eruptions. In periods when such events are absent, the correlation between continental scale temperatures typically drops substantially and in many cases resides close to 0 in both the proxies as well as model simulations. However, the model simulations, and especially the CCSM model, seem to overestimate postvolcanic cooling, particularly after the large eruptions in 1257, 1452, 1600, 1815, and 1991. The impact of particular eruptions is thus imprecisely represented in some model simulations. Nevertheless, there is also some agreement in the character of the large volcanic responses in both the proxies and models, despite the background of internal variability, as volcanic forcing synchronizes temperature variability among continents.

References

Ammann, C. M., Joos, F., Schimel, D. S., Otto-Bliesner, B. L., & Tomas, R. A. (2007). Solar influence on climate during the past millennium: Results from transient simulations with the NCAR Climate System Model. *Proceedings of the National Academy of Sciences of the United States of America*, *104*(10), 3713–3718. https://doi.org/10.1073/pnas.0605064103

Anchukaitis, K. J., Breitenmoser, P., Briffa, K. R., Buchwal, A., Büntgen, U., Cook, E. R., … Wilson, J. S. (2012). Tree rings and volcanic cooling. *Nature Geoscience*, *5*(12), 836–837. https://doi.org/10.1038/ngeo1645

Anchukaitis, K. J., Buckley, B. M., Cook, E. R., Cook, B. I., D'Arrigo, R. D., & Ammann, C. M. (2010). The influence of volcanic eruptions on the climate of the Asian monsoon region. *Geophysical Research Letters*, *37*, L22703. https://doi.org/10.1029/2010GL044843

Anchukaitis, K. J., Wilson, R., Briffa, K. R., Büntgen, U., Cook, E. R., D'Arrigo, R. D., … Zorita, E. (2017). Last millennium Northern Hemisphere summer temperatures from tree rings: Part II: Spatially resolved reconstructions. *Quaternary Science Reviews*, *163*, 1–22. https://doi.org/10.1016/j.quascirev.2017.02.020

Atwood, A. R., Wu, E., Frierson, D. M. W., & Battisti, D. S. (2016). Quantifying climate forcings and feedbacks over the last millennium in the CMIP5–PMIP3 models. *Journal of Climate*, *29*, 1161–1178. https://doi.org/10.1175/JCLI-D-15-0063.s1

Ault, T. R., Cole, J. E., Overpeck, J. T., Pederson, G. T., & Meko, D. M. (2014). Assessing the risk of persistent drought using climate model simulations and paleoclimate data. *Journal of Climate*, *27*(20), 7529–7549. https://doi.org/10.1175/JCLI-D-12-00282.1

Braconnot, P., Harrison, S. P., Kageyama, M., Bartlein, P. J., Masson-Delmotte, V., Abe-Ouchi, A., … Zhao, Y. (2012). Evaluation of climate models using palaeoclimatic data. *Nature Climate Change*, *2*(6), 417–424. https://doi.org/10.1038/nclimate1456

Briffa, K. R., Melvin, T. M., Osborn, T. J., Hantemirov, R. M., Kirdyanov, A. V., Mazepa, V. S., … Esper, J. (2013). Reassessing the evidence for tree-growth and inferred temperature change during the Common Era in Yamalia, northwest Siberia. *Quaternary Science Reviews*, *72*, 83–107. https://doi.org/10.1016/j.quascirev.2013.04.008

Briffa, K. R., Shishov, V. V., Melvin, T. M., Vaganov, E. A., Grudd, H., Hantemirov, R. M., … Naurzbaev, M. M. (2008). Trends in recent temperature and radial tree growth spanning 2000 years across northwest Eurasia. *Philosophical Transactions of the Royal Society of London. Series B, Biological Sciences*, *363*(1501), 2271–2284. https://doi.org/10.1098/rstb.2007.2199

Brohan, P., Allan, R., Freeman, E., Wheeler, D., Wilkinson, C., & Williamson, F. (2012). Constraining the temperature history of the past millennium using early instrumental observations. *Climate of the Past*, *8*(5), 1551–1563. https://doi.org/10.5194/cp-8-1551-2012

Büntgen, U., Esper, J., Frank, D., Nicolussi, K., & Schmidhalter, M. (2005). A 1052-year tree-ring proxy for Alpine summer temperatures. *Climate Dynamics*, *25*(2–3), 141–153. https://doi.org/10.1007/s00382-005-0028-1

Büntgen, U., Frank, D., Carrer, M., Urbinati, C., & Esper, J. (2009). Improving Alpine summer temperature reconstructions by increasing sample size. *Trace*, *7*, 36–43.

Büntgen, U., Frank, D., Neuenschwander, T., & Esper, J. (2012). Fading temperature sensitivity of Alpine tree growth at its Mediterranean margin and associated effects on large-scale climate reconstructions. *Climatic Change*, *114*(3–4), 651–666. https://doi.org/10.1007/s10584-012-0450-4

Büntgen, U., Frank, D., Nievergelt, D., & Esper, J. (2006). Summer temperature variations in the European Alps, A.D. 755–2004. *Journal of Climate*, *19*, 5606–5623.

Büntgen, U., Kyncl, T., Ginzler, C., Jacks, D. S., Esper, J., Tegel, W., & Heußner, K.-U. (2013). Filling the Eastern European gap in millennium-long temperature reconstructions. *Proceedings of the National Academy of Sciences of the United States of America*, *110*(5), 1773–1778. https://doi.org/10.1073/pnas.1211485110

Büntgen, U., Myglan, V. S., Ljungqvist, F. C., McCormick, M., Di Cosmo, N., Sigl, M., … Kirdyanov, A. V. (2016). Cooling and societal change during the Late Antique Little Ice Age from 536 to around 660 AD. *Nature Geoscience*, *9*(3), 231–236. https://doi.org/10.1038/ngeo2652

Büntgen, U., Tegel, W., Nicolussi, K., McCormick, M., Frank, D., Trouet, V., … Esper, J. (2011). 2500 Years of European climate variability and human susceptibility. *Science*, *331*(6017), 578–582. https://doi.org/10.1126/science.1197175

Büntgen, U., Trnka, M., Krusic, P. J., Kyncl, T., Kyncl, J., Luterbacher, J., … Esper, J. (2015). Tree-ring amplification of the early nineteenth-century summer cooling in Central Europe. *Journal of Climate*, *28*(13), 5272–5288. https://doi.org/10.1175/JCLI-D-14-00673.1

Christiansen, B. (2011). Reconstructing the NH mean temperature: Can underestimation of trends and variability be avoided? *Journal of Climate*, *24*(3), 674–692. https://doi.org/10.1175/2010JCLI3646.1

Christiansen, B., & Ljungqvist, F. C. (2017). Challenges and perspectives for large-scale temperature reconstructions of the past two millennia. *Reviews of Geophysics*, *55*, 40–96. https://doi.org/10.1002/2016RG000521

Coats, S., Cook, B. I., Smerdon, J. E., & Seager, R. (2015). North American pancontinental droughts in model simulations of the last millennium*. *Journal of Climate*, *28*(5), 2025–2043. https://doi.org/10.1175/JCLI-D-14-00634.1

Coats, S., Smerdon, J. E., Cook, B. I., & Seager, R. (2015). Are simulated megadroughts in the North American Southwest forced? *Journal of Climate*, *28*(1), 124–142. https://doi.org/10.1175/JCLI-D-14-00071.1

Coats, S., Smerdon, J. E., Seager, R., Griffin, D., & Cook, B. I. (2015). Winter-to-summer precipitation phasing in southwestern North America: A multicentury perspective from paleoclimatic model-data comparisons. *Journal of Geophysical Research: Atmospheres*, *120*, 8052–8064. https://doi.org/10.1002/2015JD023085

Cole-Dai, J., Ferris, D., Lanciki, A., Savarino, J., Baroni, M., & Thiemens, M. H. (2009). Cold decade (AD 1810–1819) caused by Tambora (1815) and another (1809) stratospheric volcanic eruption. *Geophysical Research Letters*, *36*, L22703. https://doi.org/10.1029/2009GL040882

Colose, C. M., LeGrande, A. N., & Vuille, M. (2016). Hemispherically asymmetric volcanic forcing of tropical hydroclimate during the last millennium. *Earth System Dynamics*, *7*(3), 681–696. https://doi.org/10.5194/esd-7-681-2016

Cowtan, K., & Way, R. G. (2014). Coverage bias in the HadCRUT4 temperature series and its impact on recent temperature trends. *Quarterly Journal of the Royal Meteorological Society*, *140*(683), 1935–1944. https://doi.org/10.1002/qj.2297

Crowley, T. J., & Unterman, M. B. (2013). Technical details concerning development of a 1200 yr proxy index for global volcanism. *Earth System Science Data*, *5*(1), 187–197. https://doi.org/10.5194/essd-5-187-2013

D'Arrigo, R. D., Jacoby, G. C., Frank, D., Pederson, N., Cook, E. R., Buckley, B. M., … Dugarjav, C. (2001). 1738 years of Mongolian temperature variability inferred from a tree-ring width chronology of Siberian pine. *Geophysical Research Letters*, *28*(3), 543–546. https://doi.org/10.1029/2000GL011845

D'Arrigo, R. D., Wilson, R. J. S., & Anchukaitis, K. J. (2013). Volcanic cooling signal in tree ring temperature records for the past millennium. *Journal of Geophysical Research: Atmospheres*, *118*, 9000–9010. https://doi.org/10.1002/jgrd.50692

Davi, N. K., D'Arrigo, R. D., Jacoby, G. C., Cook, E. R., Anchukaitis, K. J., Nachin, B., … Leland, C. (2015). A long-term context (931–2005 C.E.) for rapid warming over Central Asia. *Quaternary Science Reviews*, *121*, 89–97. https://doi.org/10.1016/j.quascirev.2015.05.020

Dufresne, J.-L., Foujols, M.-A., Denvil, S., Caubel, A., Marti, O., Aumont, O., … Vuichard, N. (2013). Climate change projections using the IPSL-CM5 Earth System Model: From CMIP3 to CMIP5. *Climate Dynamics*, *40*(9–10), 2123–2165. https://doi.org/10.1007/s00382-012-1636-1

Esper, J., Büntgen, U., Hartl-Meier, C., Oppenheimer, C., & Schneider, L. (2017). Northern Hemisphere temperature anomalies during the 1450s period of ambiguous volcanic forcing. *Bulletin of Volcanology*, *79*, 41. https://doi.org/10.1007/s00445-017-1125-9

Esper, J., Büntgen, U., Luterbacher, J., & Krusic, P. (2013). Testing the hypothesis of post-volcanic missing rings in temperature sensitive dendrochronological data. *Dendrochronologia*, *13*, 216–222. https://doi.org/10.1016/j.dendro.2012.11.002

Esper, J., Frank, D., Timonen, M., Zorita, E., Wilson, R. J. S., Luterbacher, J., … Büntgen, U. (2012). Orbital forcing of tree-ring data. *Nature Climate Change*, *2*(12), 862–866. https://doi.org/10.1038/NCLIMATE1589

Esper, J., Frank, D. C., Wilson, R. J. S., & Briffa, K. R. (2005). Effect of scaling and regression on reconstructed temperature amplitude for the past millennium. *Geophysical Research Letters*, *32*, L07711. https://doi.org/10.1029/2004GL021236

Esper, J., Krusic, P. J., Ljungqvist, F. C., Luterbacher, J.,Carrer, M., Cook, E. R., … Büntgen, U. (2016). Ranking of tree-ring based temperature reconstructions of the past millennium. *Quaternary Science Reviews*, *145*, 134–151. https://doi.org/10.1016/j.quascirev.2016.05.009

Esper, J., Schneider, L., Krusic, P. J., Luterbacher, J., Büntgen, U., Timonen, M., … Zorita, E. (2013). European summer temperature response to annually dated volcanic eruptions over the past nine centuries. *Bulletin of Volcanology*, *75*(7). https://doi.org/10.1007/s00445-013-0736-z

Esper, J., Schneider, L., Smerdon, J. E., Schöne, B. R., & Büntgen, U. (2015). Signals and memory in tree-ring width and density data. *Dendrochronologia*, *35*, 62–70. https://doi.org/10.1016/j.dendro.2015.07.001

Esper, J., Schweingruber, F. H., & Winiger, M. (2002). 1300 years of climatic history for Western Central Asia inferred from tree-rings. *The Holocene*, *12*(3), 267–277. https://doi.org/10.1191/0959683602hl543rp

Esper, J., Shiyatov, S. G., Mazepa, V. S., Wilson, R. J. S., Graybill, D. A., & Funkhouser, G. (2003). Temperature-sensitive Tien Shan tree ring chronologies show multi-centennial growth trends. *Climate Dynamics*, *21*(7–8), 699–706. https://doi.org/10.1007/s00382-003-0356-y

Fernández-Donado, L., González-Rouco, J. F., Raible, C. C., Ammann, C. M., Barriopedro, D., García-Bustamante, E., … Zorita, E. (2013). Large-scale temperature response to external forcing in simulations and reconstructions of the last millennium. *Climate of the Past*, *9*(1), 393–421. https://doi.org/10.5194/cp-9-393-2013

Frank, D., Esper, J., Zorita, E., & Wilson, R. J. S. (2010). A noodle, hockey stick, and spaghetti plate: A perspective on high-resolution paleo-climatology. *WIREs Climate Change*, *1*(4), 507–516. https://doi.org/10.1002/wcc.53

Gao, C., Robock, A., & Ammann, C. M. (2008). Volcanic forcing of climate over the past 1500 years: An improved ice core-based index for climate models. *Journal of Geophysical Research*, *113*, D23111. https://doi.org/10.1029/2008JD010239

Gennaretti, F., Arseneault, D., Nicault, A., Perreault, L., & Begin, Y. (2014). Volcano-induced regime shifts in millennial tree-ring chronologies from northeastern North America. *Proceedings of the National Academy of Sciences of the United States of America*, *111*(28), 10,077–10,082. https://doi.org/10.1073/pnas.1324220111

Graumlich, L. J. (1993). A 1000-year record of temperature and precipitation in the Sierra Nevada. *Quaternary Research*, *39*(2), 249–255. https://doi.org/10.1006/qres.1993.1029

Guillet, S., Corona, C., Stoffel, M., Khodri, M., Lavigne, F., Ortega, P., … Oppenheimer, C. (2017). Climate response to the Samalas volcanic eruption in 1257 revealed by proxy records. *Nature Geoscience*, *10*, 123–128. https://doi.org/10.1038/NGEO2875

Harrison, S. P., Bartlein, P. J., & Prentice, I. C. (2016). What have we learnt from palaeoclimate simulations? *Journal of Quaternary Science*, *31*(4), 363–385. https://doi.org/10.1002/jqs.2842

Hegerl, G. C., Crowley, T. J., Hyde, W. T., & Frame, D. J. (2006). Climate sensitivity constrained by temperature reconstructions over the past seven centuries. *Nature*, *440*(7087), 1029–1032. https://doi.org/10.1038/nature04679

Helama, S., Fauria, M. M., Mielikäinen, K., Timonen, M., & Eronen, M. (2010). Sub-Milankovitch solar forcing of past climates: Mid and late Holocene perspectives. *Geological Society of America Bulletin*, *122*(11–12), 1981–1988. https://doi.org/10.1130/B30088.1

Helama, S., Vartiainen, M., Holopainen, J., Mäkelä, H., Kolström, T., & Meriläinen, J. (2014). A palaeotemperature record for the Finnish Lakeland based on microdensitometric variations in tree rings. *Geochronometria*, *41*(3), 265–277. https://doi.org/10.2478/s13386-013-0163-0

Jungclaus, J. H., Bard, E., Baroni, M., Braconnot, P., Cao, J., Chini, L. P., … Zorita, E. (2016). The PMIP4 contribution to CMIP6—Part 3: The last millennium, scientific objective and experimental design for the PMIP4 past1000 simulations. *Geoscientific Model Development Discussion*, *2016*, 1–34. https://doi.org/10.5194/gmd-2016-278

Jungclaus, J. H., Lohmann, K., & Zanchettin, D. (2014). Enhanced 20th-century heat transfer to the Arctic simulated in the context of climate variations over the last millennium. *Climate of the Past*, *10*(6), 2201–2213. https://doi.org/10.5194/cp-10-2201-2014

Landrum, L., Otto-Bliesner, B. L., Wahl, E. R., Conley, A., Lawrence, P. J., Rosenbloom, N., & Teng, H. (2013). Last millennium climate and its variability in CCSM4. *Journal of Climate*, *26*(4), 1085–1111. https://doi.org/10.1175/JCLI-D-11-00326.1

Linderholm, H. W., & Gunnarson, B. E. (2005). Summer temperature variability in central Scandinavia during the last 3600 years. *Geografiska Annaler A*, *87*(1), 231–241. https://doi.org/10.1111/j.0435-3676.2005.00255.x

Liu, Y., An, Z., Linderholm, H. W., Chen, D., Song, H., Cai, Q., … Tian, H. (2009). Annual temperatures during the last 2485 years in the mid-eastern Tibetan Plateau inferred from tree rings. *Science in China, Series D: Earth Sciences*, *52*(3), 348–359. https://doi.org/10.1007/s11430-009-0025-z

Ljungqvist, F. C., Krusic, P. J., Sundqvist, H. S., Zorita, E., Brattström, G., & Frank, D. (2016). Northern Hemisphere hydroclimate variability over the past twelve centuries. *Nature*, *532*(7597), 94–98. https://doi.org/10.1038/nature17418

Lloyd, A. H., & Graumlich, L. J. (1997). Holocene dynamics of treeline forests in the Sierra Nevada. *Ecology*, *78*(4), 1199–1210. https://doi.org/10.2307/2265869

Luckman, B. H., & Wilson, R. J. S. (2005). Summer temperatures in the Canadian Rockies during the last millennium: A revised record. *Climate Dynamics*, *24*(2–3), 131–144. https://doi.org/10.1007/s00382-004-0511-0

Luterbacher, J., Werner, J. P., Smerdon, J. E., Fernández-Donado, L., González-Rouco, F. J., Barriopedro, D., … Zerefos, C. (2016). European summer temperatures since Roman times. *Environmental Research Letters*, *11*(2), 024001. https://doi.org/10.1088/1748-9326/11/2/024001

Mann, M. E. (2002). Climate reconstruction. The value of multiple proxies. *Science*, *297*(5586), 1481–1482. https://doi.org/10.1126/science.1074318

Mann, M. E., Fuentes, J. D., & Rutherford, S. (2012). Underestimation of volcanic cooling in tree-ring-based reconstructions of hemispheric temperatures. *Nature Geoscience*, *5*(3), 202–205. https://doi.org/10.1038/ngeo1394

Mann, M. E., Rutherford, S., Schurer, A. P., Tett, S. F. B., & Fuentes, J. D. (2013). Discrepancies between the modeled and proxy-reconstructed response to volcanic forcing over the past millennium: Implications and possible mechanisms. *Journal of Geophysical Research – Atmospheres*, *118*, 7617–7627. https://doi.org/10.1002/jgrd.50609

Marotzke, J., & Forster, P. M. (2015). Forcing, feedback and internal variability in global temperature trends. *Nature*, *517*(7536), 565–570. https://doi.org/10.1038/nature14117

Masson-Delmotte, V., Schulz, M., Abe-Ouchi, A., Beer, J., Ganopolski, J., González Rouco, J. F., … Timmermann, A. (2013). Information from paleoclimate archives. In *Climate change 2013: The physical science basis*. Contribution of Working Group I to the Fifth Assessment Report of the Intergovernmental Panel on Climate Change (pp. 383–464). Cambridge, UK, New York, NY: Cambridge University Press.

McKay, N. P., & Kaufman, D. S. (2014). An extended Arctic proxy temperature database for the past 2,000 years. *Scientific Data*, *1*, 140026. https://doi.org/10.1038/sdata.2014.26

Melvin, T. M., Grudd, H., & Briffa, K. R. (2013). Potential bias in 'updating' tree-ring chronologies using regional curve standardisation: Re-processing 1500 years of Torneträsk density and ring-width data. *The Holocene*, *23*(3), 364–373. https://doi.org/10.1177/0959683612460791

Morice, C. P., Kennedy, J. J., Rayner, N. A., & Jones, P. D. (2012). Quantifying uncertainties in global and regional temperature change using an ensemble of observational estimates: The HadCRUT4 data set. *Journal of Geophysical Research*, *117*, D08101. https://doi.org/10.1029/2011JD017187

Myglan, V. S., Oidupaa, O. C., & Vaganov, E. A. (2012). A 2367-year tree-ring chronology for the Altai–Sayan region (Mongun-Taiga mountain massif). *Archaeology, Ethnology and Anthropology of Eurasia*, *40*, 76–83.

Myglan, V. S., Zharnikova, O. A., Malysheva, N. V., Gerasimova, O. V., Vaganov, E. A., & Sidorov, O. V. (2012). Constructing the tree-ring chronology and reconstructing summertime air temperatures in southern Altai for the last 1500 years. *Geography and Natural Resources*, *33*(3), 200–207. https://doi.org/10.1134/S1875372812030031

Otto-Bliesner, B. L., Brady, E. C., Fasullo, J., Jahn, A., Landrum, L., Stevenson, S., … Strand, G. (2016). Climate variability and change since 850 CE: An ensemble approach with the Community Earth System Model. *Bulletin of the American Meteorological Society*, *97*(5), 735–754. https://doi.org/10.1175/bams-d-14-00233.1

PAGES 2k Consortium (2013). Continental-scale temperature variability during the past two millennia. *Nature Geoscience*, *6*(6), 339–346. https://doi.org/10.1038/ngeo1834

PAGES 2k-PMIP3 group (2015). Continental-scale temperature variability in PMIP3 simulations and PAGES 2k regional temperature reconstructions over the past millennium. *Climate of the Past*, *11*(12), 1673–1699. https://doi.org/10.5194/cp-11-1673-2015

Robock, A. (2000). Volcanic eruptions and climate. *Reviews of Geophysics*, *38*(2), 191–219. https://doi.org/10.1029/1998RG000054

Salzer, M. W., & Kipfmueller, K. F. (2005). Reconstructed temperature and precipitation on a millennial timescale from tree-rings in the Southern Colorado Plateau, U.S.A. *Climatic Change*, *70*(3), 465–487. https://doi.org/10.1007/s10584-005-5922-3

Salzer, M. W., Bunn, A. G., Graham, N. E., & Hughes, M. K. (2014). Five millennia of paleotemperature from tree-rings in the Great Basin, USA. *Climate Dynamics*, *42*(5–6), 1517–1526. https://doi.org/10.1007/s00382-013-1911-9

Schmidt, G. A. (2010). Enhancing the relevance of palaeoclimate model/data comparisons for assessments of future climate change. *Journal of Quaternary Science*, *25*(1), 79–87. https://doi.org/10.1002/jqs.1314

Schmidt, G. A., Annan, J. D., Bartlein, P. J., Cook, B. I., Guilyardi, E., Hargreaves, J. C., … Yiou, P. (2014). Using palaeo-climate comparisons to constrain future projections in CMIP5. *Climate of the Past*, *10*(1), 221–250. https://doi.org/10.5194/cp-10-221-2014

Schmidt, G. A., Jungclaus, J. H., Ammann, C. M., Bard, E., Braconnot, P., Crowley, T. J., … Vieira, L. E. A. (2011). Climate forcing reconstructions for use in PMIP simulations of the last millennium (v1.0). *Geoscientific Model Development*, *4*(1), 33–45. https://doi.org/10.5194/gmd-4-33-2011

Schneider, L., Smerdon, J. E., Büntgen, U., Wilson, R. J. S., Myglan, V. S., Kirdyanov, A. V., & Esper, J. (2015). Revising midlatitude summer temperatures back to A.D. 600 based on a wood density network. *Geophysical Research Letters*, *42*, 4556–4562. https://doi.org/10.1002/2015GL063956

Schneider, L., Smerdon, J. E., Pretis, F., Hartl-Meier, C., & Esper, J. (2017). An independent record of large volcanic events over the past millennium from reconstructed summer temperatures. *Environmental Research Letters*, *12*, 094005. https://doi.org/10.1088/1748-9326/aa7a1b

Schurer, A. P., Hegerl, G. C., Mann, M., Tett, S. F. B., & Phipps, S. J. (2013). Separating forced from chaotic climate variability over the past millennium. *Journal of Climate*, *26*, 6954–6973. https://doi.org/10.1175/JCLI-D-12-00826.1

Schurer, A. P., Tett, S. F. B., & Hegerl, G. C. (2014). Small influence of solar variability on climate over the past millennium. *Nature Geoscience*, *7*(2), 104–108. https://doi.org/10.1038/ngeo2040

Schweingruber, F. H., Bartholin, T., Schär, E., & Briffa, K. R. (1988). Radiodensitometric-dendroclimatological conifer chronologies from Lapland (Scandinavia) and the Alps (Switzerland). *Boreas*, *17*(4), 559–566.

Sidorova, O. V., Naurzbaev, M. M., & Vaganov, E. A. (2006). An integral estimation of tree-ring chronologies from subarctic regions of Eurasia. *Trace*, *4*, 84–91.

Sigl, M., Winstrup, M., McConnell, J. R., Welten, K. C., Plunkett, G., Ludlow, F., … Woodruff, T. E. (2015). Timing and climate forcing of volcanic eruptions for the past 2,500 years. *Nature*, *523*(7562), 543–549. https://doi.org/10.1038/nature14565

Smerdon, J. E., & Pollack, H. N. (2016). Reconstructing Earth's surface temperature over the past 2000 years: The science behind the headlines. *WIREs Climate Change*, *7*, 746–771. https://doi.org/10.1002/wcc.418

Smerdon, J. E., Coats, S., & Ault, T. R. (2016). Model-dependent spatial skill in pseudoproxy experiments testing climate field reconstruction methods for the Common Era. *Climate Dynamics*, *46*(5), 1921–1942. https://doi.org/10.1007/s00382-015-2684-0

Smerdon, J. E., Kaplan, A., Zorita, E., González-Rouco, J. F., & Evans, M. N. (2011). Spatial performance of four climate field reconstruction methods targeting the Common Era. *Geophysical Research Letters*, *38*, L11705. https://doi.org/10.1029/2011GL047372

Smerdon, J. E., Luterbacher, J., Phipps, S. J., Anchukaitis, K. J., Ault, T., Coats, S., … Xoplak, E. (2017). Comparing proxy and model estimates of hydroclimate variability and change over the Common Era. *Climate of the Past Discussions*, *2017*, 1–70. https://doi.org/10.5194/cp-2017-37

Snyder, C. W. (2010). The value of paleoclimate research in our changing climate. *Climatic Change*, *100*(3–4), 407–418. https://doi.org/10.1007/s10584-010-9842-5

St. George, S., Ault, T. R., & Torbenson, M. C. A. (2013). The rarity of absent growth rings in Northern Hemisphere forests outside the American Southwest. *Geophysical Research Letters*, *40*, 3727–3731. https://doi.org/10.1002/grl.50743

Stoffel, M., Khodri, M., Corona, C., Guillet, S., Poulain, V., Bekki, S., … Masson-Delmotte, V. (2015). Estimates of volcanic-induced cooling in the Northern Hemisphere over the past 1,500 years. *Nature Geoscience*, *8*(10), 784–788. https://doi.org/10.1038/ngeo2526

von Storch, H., Zorita, E., Jones, J. M., Dimitriev, Y., González-Rouco, J. F., & Tett, S. F. B. (2004). Reconstructing past climate from noisy data. *Science*, *306*(5696), 679–682. https://doi.org/10.1126/science.1096109

Taylor, K. E., Stouffer, R. J., & Meehl, G. A. (2012). An overview of CMIP5 and the experiment design. *Bulletin of the American Meteorol Society*, *93*(4), 485–498. https://doi.org/10.1175/BAMS-D-11-00094.1

Tingley, M. P., Craigmile, P. F., Haran, M., Li, B., Mannshardt, E., & Rajaratnam, B. (2012). Piecing together the past: Statistical insights into paleoclimatic reconstructions. *Quaternary Science Reviews*, *35*, 1–22. https://doi.org/10.1016/j.quascirev.2012.01.012

Valdes, P. (2011). Built for stability. *Nature Geoscience*, *4*(7), 414–416. https://doi.org/10.1038/ngeo1200

Wang, J., Yang, B., Qin, C., Kang, S., He, M., & Wang, Z. (2014). Tree-ring inferred annual mean temperature variations on the southeastern Tibetan Plateau during the last millennium and their relationships with the Atlantic Multidecadal Oscillation. *Climate Dynamics*, *43*(3–4), 627–640. https://doi.org/10.1007/s00382-013-1802-0

Wiles, G., D'Arrigo, R. D., Barclay, D., Wilson, R. J. S., Jarvis, S. K., Vargo, L., & Frank, D. (2014). Surface air temperature variability reconstructed with tree rings for the Gulf of Alaska over the past 1200 years. *The Holocene*, *24*(2), 198–208. https://doi.org/10.1177/0959683613516815

Wilson, R. J. S., Anchukaitis, K., Briffa, K. R., Büntgen, U., Cook, E., D'Arrigo, R., … Zorita, E. (2016). Last millennium Northern Hemisphere summer temperatures from tree rings: Part I: The long term context. *Quaternary Science Reviews*, *134*, 1–18. https://doi.org/10.1016/j.quascirev.2015.12.005

Wu, T., Yu, R., Zhang, F., Wang, Z., Dong, M., Wang, L., … Li, L. (2010). The Beijing Climate Center atmospheric general circulation model: Description and its performance for the present-day climate. *Climate Dynamics*, *34*(1), 123–147. https://doi.org/10.1007/s00382-008-0487-2

Yadav, R. R., Braeuning, A., & Singh, J. (2011). Tree ring inferred summer temperature variations over the last millennium in western Himalaya, India. *Climate Dynamics*, *36*(7–8), 1545–1554. https://doi.org/10.1007/s00382-009-0719-0

Zhang, Y., Shao, X., Yin, Z.-Y., & Wang, Y. (2014). Millennial minimum temperature variations in the Qilian Mountains, China: Evidence from tree rings. *Climate of the Past*, *10*(5), 1763–1778. https://doi.org/10.5194/cp-10-1763-2014

Zhu, H., Zheng, Y., Shao, X., Liu, X., Xu, Y., & Liang, E. (2008). Millennial temperature reconstruction based on tree-ring widths of Qilian juniper from Wulan, Qinghai Province, China. *Scientific Bulletin*, *53*(24), 3914–3920. https://doi.org/10.1007/s11434-008-0400-8